*Korean J. Chem. Eng.*, 32(1), 159-167 (2015)
DOI: 10.1007/s11814-014-0218-9

pISSN: 0256-1115
eISSN: 1975-7220

# Experimental and computational investigation of polyacrylonitrile ultrafiltration membrane for industrial oily wastewater treatment

**Hooman Adib[*,**], Shadi Hassanajili[*,†], Mohammad Reza Sheikhi-Kouhsar[*], Abdolhamid Salahi[***], and Toraj Mohammadi[***]**

*Department of Chemical Engineering, School of Chemical and Petroleum Engineering, Shiraz University, Shiraz, Iran
**National Iranian Gas Company (NIGC), South Pars Gas Complex (SPGC), Asaluyeh, Iran
***Research Centre for Membrane Separation Processes (RCMSP), Faculty of Chemical Engineering, Iran University of Science and Technology (IUST), Narmak, Tehran 16846, Iran
(*Received 14 March 2014 • accepted 30 July 2014*)

**Abstract**−An experimental study on separation of industrial oil from oily wastewater has been done. A polyacrylonitrile membrane with a molecular weight cut-off (MWCO) of 20 kDa was used and an outlet wastewater of API unit of Tehran refinery was employed. The main purpose of this study was to develop a support vector machine model for permeation flux decline and fouling resistance in a cross-flow hydrophilic polyacrylonitrile membrane during ultrafiltration. The operating conditions which have been applied to develop a support vector machine model were transmembrane pressure (TMP), operating temperature, cross flow velocity (CFV), pH values of oily wastewater, permeation flux decline and fouling resistance. The testing results obtained by the support vector machine models are in very good agreement with experimental data. The calculated squared correlation coefficients for permeation flux decline and fouling resistance were both 0.99. Based on the results, the support vector machine proved to be a reliable accurate estimation method.

Keywords: Polyacrylonitrile, Permeation Flux Decline, Fouling Resistance, Support Vector Machine, Tehran Refinery

## INTRODUCTION

Oily wastewaters are one of the most important sources of pollutant emitted into water by industrial and domestic sewage. They have become a major threat to water sources and environment that must be solved urgently. Many customary methods are used for separation of oily wastewater [1-4]. One of the treatment techniques which receives significant attention in related industries is membrane filtration.

The most important advantages of membrane processes would be the lower capital cost and the absence of chemical addition and subsequent generation of oily sludge [5, 6]. In recent years, ultrafiltration (UF) membrane technology has gained tremendous importance for purification of drinking water and oily wastewaters [7-9]. One of the commercial ultrafiltration membranes commonly used is polyacrylonitrile (PAN) membrane. PAN has been used in the preparation of UF membranes for a long time due to its superior resistance to hydrolysis and oxidation. One of the problems which a PAN membrane usually encounters is fouling, especially organic fouling and bio-fouling, which may result in a severe decline in their permeability and rejection performance over a period of operation [10,11]. The fouling in membranes causes higher operating pressure requirement, limited recoveries, feed water loss, frequent chemical cleaning, declining permeation flux and short lifetimes of membranes [12-14]. Some mechanisms of membrane fouling have been mentioned as follows [6]:

a. Adsorption inside the membrane
b. Blocking of the membrane pores
c. High concentration of foulants near the membrane, concentration polarization
d. Deposition on the membrane surface forming a cake/gel layer
e. Compression of the cake/gel layer

For membrane filtration, these mechanisms may occur simultaneously. Membrane fouling is very complex and difficult to model, and no quality parameters exist by which this rate of fouling and permeation flux decline can be predicted accurately [15-18]. During constant-pressure ultrafiltration of the oily wastewater, the permeation flux will continue to decrease while the filtration resistance will continue to increase with filtration time due to accumulation of foulants on the membrane surface. Membrane fouling can cause severe flux decline and affect the quality of the water produced, which this phenomena could be mentioned as permeation flux decline.

Many authors have used black box models for modeling membrane processes. Attempts to develop such models include those based on basic principles and those that are data-based using input/output experimental data. Models based on detailed mass and energy balance equations proved to be very complicated and hard to solve, especially when coupled with optimization computer routines. Available commercial simulation softwares that are not open-source can be used to perform accurate simulations. Moreover, the proprietary nature of these softwares is another encouragement to their appli-

†To whom correspondence should be addressed.
E-mail: ajili@shirazu.ac.ir

cation. Such computer based models can now be applicable for many membrane processes such as Shokrkar et al. [19], who predicted permeation flux decline using genetic programming. The results obtained from the genetic programming model demonstrated good representation of the experimental data with an average error of less than 5%. Hwang et al. [20] predicted membrane fouling in a microfiltration system using genetic programming. The developed model allows predicting satisfactorily the filtration performance of the pilot plant obtained for different water quality and changing operating conditions; and the result indicated that genetic programming has potential to assess membrane performance as an "intelligent" membrane system. Liu et al. [21] used artificial neural networks to develop a model for membrane fouling. The effects of operating parameters on membrane performance were evaluated based on the comparison of trans-membrane pressure (TMP) as a function of operating time. Madaeni and Kurdian [22] used fuzzy logic modeling and hybrid genetic algorithm (GA) optimization of virus removal from water using microfiltration. It was observed that the fuzzy inference system (FIS) predicts rejection and flux during microfiltration for different operating conditions with an acceptable error.

In this study an experimental investigation on separation of oil from oily wastewater in a cross-flow hydrophilic PAN membrane during ultrafiltration process was evaluated. The main aim of this study was to propose a novel approach based on the support vector machine (SVM) method to predict the permeation flux decline and fouling resistance of a PAN membrane during cross-flow ultrafiltration of oily wastewater. Four parameters such as trans-membrane pressure, operating temperature, cross flow velocity and pH value of oily wastewater could be affecting the PAN membrane during the ultrafiltration process. However, the collected experimental data cannot be examined easily to capture relevant input/output relationships because a nonlinear relation exists between parameters that somehow are very hard to obtain. Therefore, SVM as a new approach has been applied for prediction of fouling and permeation flux decline with high accuracy, which could reveal some of the application potentials of this approach as a modeling tool in membrane separation. Also, the model was evaluated for the first time to predict the fouling resistance and permeation flux decline of a PAN membrane using SVM technique.

## EXPERIMENTAL

### 1. Process Feed

Industrial oily wastewater from Tehran oil refining company was employed as feed. These wastewaters are a two-phase dispersive system in which the continuous phase is water and the dispersed phase is oil grease, total suspended solid (TSS), lubricants, cutting liquids, heavy hydrocarbons (tars, crude oils, grease and diesel oil), and light hydrocarbons (kerosene, jet fuel and gasoline) and chemical substances such as detergents, salts and caustic soda. Their amounts depend on the type of the process that generates the effluent. For these experiments, the feed was taken daily and used immediately. Analysis of the feed taken from the industrial oily wastewater before and after ultrafiltration process is presented in Table 1. Variation of the characteristics during workdays due to the different properties of inlet petroleum was not significant. Therefore, all feeds and parameters were measured three times and the average values of these parameters were used. Standard deviations were under 8%. Also, the zeta potential was measured (using a Zetasizer Nano ZS (Malvern, UK)) to calculate the charge of oil emulsion. The charge of the oily wastewaters collected from industrial oily wastewater effluent was +21.4 mV. The emulsion stability increases with absolute value of the zeta potential. According to the value of +21.4 mV for the emulsion charge, the industrial oily wastewater is stable.

**Table 1. Characteristics of the oily wastewater in the feed and after ultrafiltration process**

| Parameter | Unit | Feed | Ultrafiltration |
|---|---|---|---|
| TSS | mg/L | 250 | Trace |
| TDS | mg/L | 8200 | 4560 |
| Content of oil & grease | mg/L | 196 | 0.1 |
| COD | mg/L | 456 | 90 |
| TOC | mg/L | 150 | 36 |
| Turbidity | NTU | 260 | 0.4 |
| Total hardness (mg $CaCO_3$) | mg/L | 4620 | 2150 |
| $SiO_2$ | mg/L | 86 | 24 |

### 2. Membrane

The membrane used in the experiments was a rectangular flat sheet regenerated polyacrylonitrile membrane with a molecular weight cut-off (MWCO) of 20 kDa, a surface area of 66 $cm^2$, provided by Sepro membranes of USA. All membranes were rectangular flat sheet with a size of 5.0cm×13.2 cm, installed in a stainless steel module. Fig. 1 shows the structure of the employed membrane. The PAN membrane is porous and asymmetric. It consists of a top or skin layer with a thickness of about 0.1 to 0.5 μm supported by a porous sub-layer with a thickness of about 100 to 150 μm. This membrane combines high selectivity with high permeation flux.

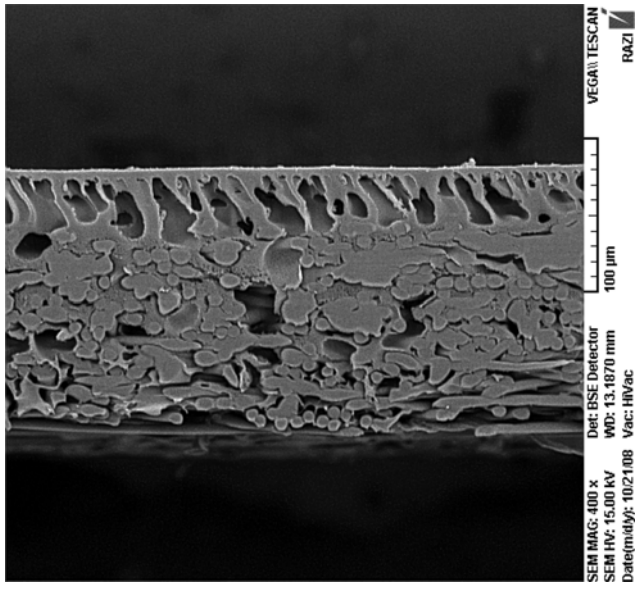


**Fig. 1. Cross sectional SEM of the PAN (20 kDa) membrane.**

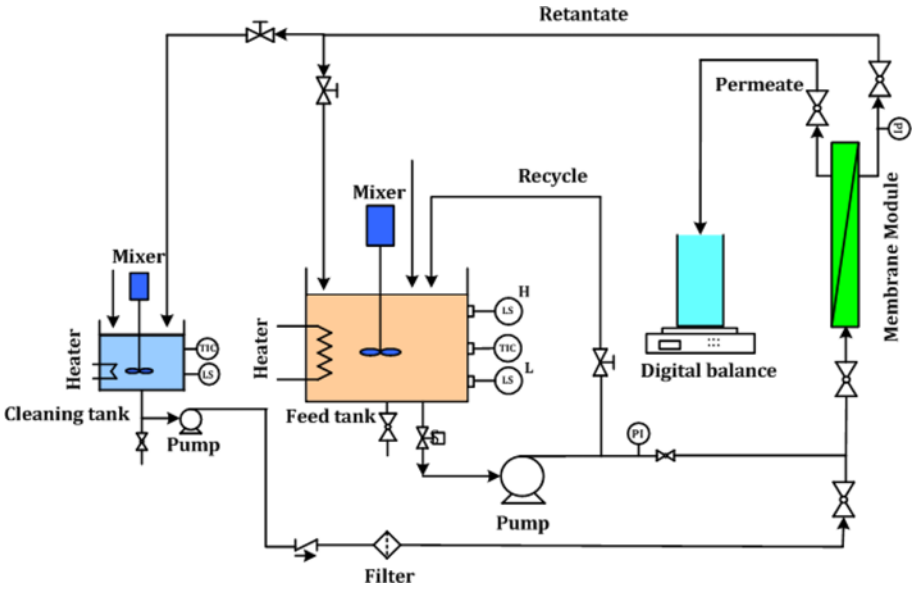


**Fig. 2. Schematic diagram of the laboratory scale cross flow filtration system.**

The results showed that the permeation flux for membrane at a trans-membrane pressure of 1 bar, temperature of 25 °C and the cross flow velocity (CFV) of 1m/s for distillated water is 800 L/m$^2$·h.

**3. Experimental Method and Procedure**

Fig. 2 shows the schematic diagram of the process of oily wastewater treatment using ultrafiltration process. As indicated, there are two operating loops in this operation. The first one is the filtration loop which refers to as cross-flow hydrophilic polyacrylonitrile membrane during ultrafiltration process, and the second one consists of chemical washing loop. The filtration system of this process includes feed tank, feed pump, chemical washing tank, temperature and level sensors, valves, pressure gage, recycle, permeate flow meters, heat exchanger and a membrane placed in a stainless steel module. The feed pump had a closed impeller with six reversed blades especially fit to transfer liquid at medium pressure to optimize the hydraulic efficiency. The cross-flow hydrophilic polyacrylonitrile membrane during ultrafiltration process was run for 6 hours. During this time, the feed pump had a maximum discharge pressure of 15 bar and a maximum capacity of 5 m$^3$/h which pumps the feed from the feed tank toward the membrane module. After that, the concentrated materials returned to the tank for subsequent filtration. Therefore, the feed concentration in the circulation loop remained virtually constant. The feed tank of this filtration system was Plexiglas, with a capacity of 50 L and two walls which allowed the feed temperature to be kept constant using the circulation of cooled and/or heated water. The membrane permeation flux was measured by collecting the permeate in an Erlenmeyer flask and using a digital balance. The inlet pressure and CFV were controlled by the by-pass and outlet valves, respectively. The cross sectional area of the membrane module was 0.75 cm$^2$ and membrane surface area in contact with fluid was 66 cm$^2$. A shell and tube type heat exchanger is included in the feed stream to control temperature. TMP and feed temperature were measured by thermocouples and pressure transducers located at the membrane inlet and outlet. Also, the recycled retentate and permeate flows were measured with variable section flow meters. The chemical washing loop was used after each experiment of oily wastewater filtration. During the experiments, CFV, TMP, feed temperature, filtration time, oil concentration and pH were carefully monitored.

**4. Analytical Methods**

Samples for measurements of the feed and the permeate total suspended solids (TSS), chemical oxygen demand (COD), oil and grease content, turbidity, total organic carbon (TOC), and total dissolved solids (TDS) (Hanna Instruments, Kehl am Rhein, Germany) were taken as necessary and analyzed by the procedure outlined in the standard methods [23]. TOC was determined using TOC analyzer (Dohrmann, model DC-190 TOC analyzer, Texas, United States). The details of the oil and grease content and TSS measurement have been described elsewhere [24]. Color measurements were conducted using HACH DR/2010 spectrophotometer. COD values were determined using HACH DR/2010. Turbidity values were estimated using a turbidimeter (Hach, model 2100A, United States). Particle size distribution of the desalter plant wastewater was measured using light scattering method by LLS instrument (MAL1008078, United Kingdom). All of the experimental analyses were accomplished at industrial and environmental protection division of research institute of petroleum industry (RIPI), IRAN.

**5. Membrane Fouling Determination**

The permeation flux of the membrane during filtration was measured using the resistance-in-series model [25].

$$J = \frac{TMP}{\mu R_t} \quad (1)$$

where J is the flux (L/m$^2$h), TMP is the trans-membrane pressure (3.5 bar), $\mu$ is the viscosity of water at room temperature and $R_t$ is the resistance encountered by water transported through the membrane. Three separate resistances need to be overcome for transport to occur through the membrane and therefore, $R_t=R_m+R_f+R_c$.

$R_m$ is the intrinsic membrane resistance; $R_f$ is the sum of the resistances caused by solute adsorption into the membrane pores or

walls and chemically reversible cake. $R_c$ is the cake resistance formed by cake layer deposited over the membrane surface due to diffusion through this layer.

$R_m$ is the special unique resistance which depends on its material, pore size and other properties. This resistance can be calculated using the initial permeate flux of distillated water ($J_{wi}$) according to Eq. (2) [24].

$$R_m = \frac{TMP}{\mu J_{wi}} \qquad (m^2/m^3) \tag{2}$$

As said above, $R_f$ is the hydraulic resistance of the adsorption inside the membrane pores, blocking of the membrane pores, deposition on the membrane surface forming a cake/gel layer, and pore plugging. This type of resistance is observed after feed filtration which can be calculated using permeate flux of distillated water after fouling and washing with water ($J_{ww}$) [24]:

$$R_f = \frac{TMP}{\mu J_{ww}} - R_m \qquad (m^2/m^3) \tag{3}$$

## THEORETICAL BACKGROUND

### 1. Support Vector Machine

Support vector machine is a universal approximator based on the structural risk minimization principle from computational learning theory [26]. SVM is a supervised learning method with associated learning algorithm that analyzes data and recognizes patterns of input/output data. Originally, SVM was developed for classification tasks [27]. It is one of the most sophisticated non-parametric supervised classifiers available today, with many different configurations depending upon the function used for generating the transform function that is commonly Kernel function. Although it is mostly considered as a linear algorithm in a high dimensional feature space, however in practice it does not involve any computations in that high dimensional space. By the use of kernels all necessary computations are performed directly in the input space [28-30].

In recent years artificial neural network (ANN) has been demonstrated to be a strong instrument to develop an estimation model between input/output data. However, in some cases it may lead to random initialization of the under development networks and variation of the stopping criteria during optimization of model parameters [31]. Other problems and limitations that the ANN approach generally has can be represented as follows:

- Extrapolation is not recommended for ANN approach
- Repeating network training hundreds of times
- Availability of large database to obtain reliable accurate results
- Tendency of ANN approach to overfit
- High dependency of final results to initial parameters.

SVM-based techniques are free of such problems and limitations, simple in their theoretical background and very powerful for developing accurate model between input/output data [32]. One of the most important advantages of SVM is that it converges to global and local optimum faster compared to ANN approach, and also there is no need to manipulate model parameters [33-35].

SVM equations are based on the statistical learning theory developed by Vapnik [36]. Given a training data set of N points $\{x_k, y_k\}$, k=1, 2, …, N, with the input data $x_k \in R^n$ and the corresponding outputs, $y_k \in R^n$, in feature space SVM model take the form:

$$y(x) = \sum_{k=1}^{N} \alpha_i . K(x, x_k) + b \tag{4}$$

where N is the number of input data having non-zero values of Lagrangian multipliers ($\alpha_i$), the nonlinear Kernel function $K(x, x_k)$ maps the input space into higher character dimension, which is calculated from the inner product of the two vectors x and $x_k$ in the feasible region built by the inner product of the vectors $\Phi(x)$ and $\Phi(x_k)$ as follows [31]:

$$K(x, x_k) = \Phi(x)^T \cdot \Phi(x_k) \tag{5}$$

b is the bias and y indicates the output vector.

Lagrangian multipliers ($\alpha_i$) can be found by solving the following quadratic programming problem [37-41]:

$$\omega(\alpha) = \sum_{i=1}^{N} \alpha_i - \frac{1}{2} \cdot \sum_{i,j=1}^{N} \alpha_i \alpha_j y_i y_j K(x_i, x_j) \tag{6}$$

Subject to constraints

$$0 \le \alpha_i \le \gamma \qquad i=1, \ldots, N$$

where $\gamma$ is user defined parameter. It controls the tradeoff between complexity of the support vector machine and the number of non-separable points and hence usually termed as a regularization parameter [29,37-41].

This compact formulation of quadratic optimization has a unique solution [42,43]. Overall, the SVM analysis takes the form of the following constrained optimization problem in order to obtain the optimum value of $\gamma$ [29,42-45]:

$$\min_{\omega, \beta, \xi_i, \xi_i^*} \frac{1}{2} \|\omega\|^2 + \gamma \cdot \sum_{i=1}^{N} (\xi_i, \xi_i^*)$$

Subject to

$$y_i - \omega^T x_i - \beta \le \varepsilon + \xi_i \qquad \forall t=1, \ldots, N$$
$$\omega^T x_i + \beta - y_i \le \varepsilon + \xi_i^* \qquad \forall t=1, \ldots, N$$
$$\xi \ge 0 \qquad \forall t=1, \ldots, N$$
$$\xi_i^* \ge 0 \qquad \forall t=1, \ldots, N$$

where $\varepsilon$ is the precision threshold, is the normal vectors of support vector machine, and $\xi_i$, $\xi_i^*$ represent the slack variables with nonnegative values to ensure feasible constraints. The first term in the objective function represents model complexity while the second term represents the model accuracy or error tolerance.

Bias, b, is usually determined by using primal constraints as:

$$b = -\left(\frac{1}{2}\right)\left[\max_{\{i, y_i=-1\}}\left(\sum_{j \in \{SV\}}^{m} y_j \alpha_j K(x_i, x_j)\right)\right] + \min_{\{i, y_i=-1\}}\left(\sum_{j \in \{SV\}}^{m} y_j \alpha_j K(x_i, x_j)\right) \tag{7}$$

where m is the number of support vectors.

In this work, the radial basis function (RBF) Kernel has been applied, which is used extensively with the following form:

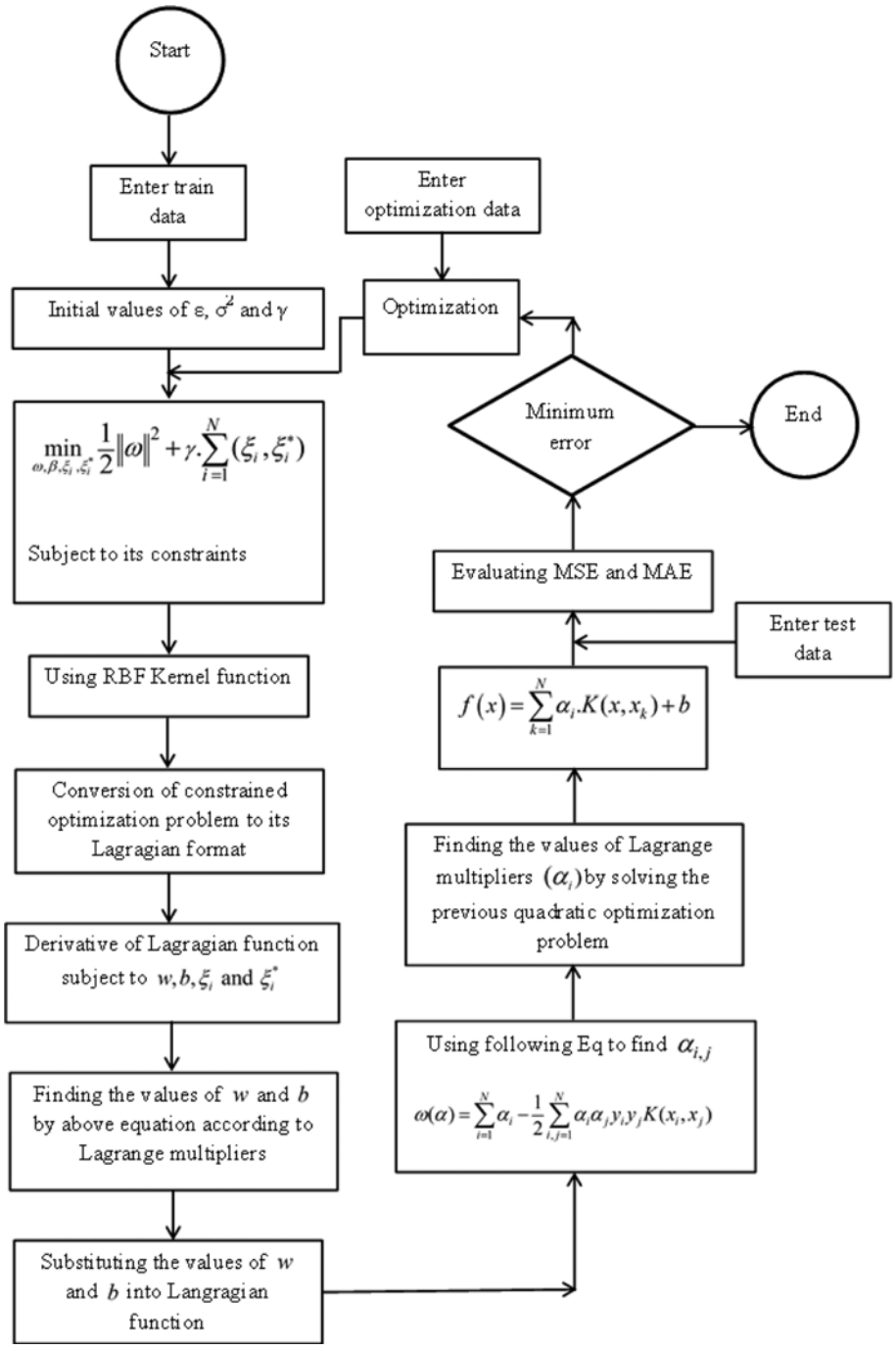


**Fig. 3. Schematic flowchart of SVM algorithm.**

$$K(x, x_k) = \exp\left(\frac{-\|x_k - x\|^2}{\sigma^2}\right) \quad (8)$$

where $\sigma$ is Kernel parameter which is treated by an external optimization algorithm during the internal SVM calculations.

The mean square error (MSE) which is used for the calculation of the error in the developed SVM models is represented as Eq. (9):

$$MSE = \frac{\sum_{i=1}^{N}(O_i - T_i)^2}{N} \quad (9)$$

where $O_i$ is the SVM-based model prediction, $T_i$ is the actual experimental data of the permeation flux decline and fouling resistance of PAN membrane and N denotes the number of the experimental data used. Also, Fig. 3 presents SVM model development procedure in flowchart format.

## MATERIALS AND METHODS

A data set of six series of input/output data each consisting 58 data of an experimental dataset is processed. All the input/output

variables have been normalized to the range [−1, +1] to prevent truncation error for model development. Eq. (10) which is used for normalizing dataset is represented as follows:

$$x_n = 2\frac{x_i - x_{min}}{x_{max} - x_{min}} - 1 \quad (10)$$

where $x_n$, $x_i$, $x_{min}$ and $x_{max}$ are the scaled value of input/output data, actual value of input/output data, minimum observation value of dataset and maximum observation value of dataset, respectively. Since input/output data to/from model are in normalized format, model outputs were recalculated to their actual values, $x_i$, by solving Eq. (10) accordingly.

To evaluate generality and robust performance of the SVM model during model development comprehensively, the normalized data set was divided down randomly into two subsets that are "training" set and "testing" set. In this study, 80% of the data is used for training and the other 20% is used for testing purpose.

## RESULTS AND DISCUSSION

### 1. Experimental Data

The total number of experimental data for the proposed model was six series, where each of the data series includes 58 data points from input/output experimental data. The available data are trans-membrane pressure, operating temperature, cross-flow velocity, pH values of oily wastewater, permeation flux decline and fouling resistance of a PAN membrane. Table 2 shows the range of experimental data used in this research. Also, a full description of experimental investigation of the present paper is given in our previous work [6].

**Table 2. Range of dataset used for input/output of SVM algorithm**

| Measured variables | | Min | Max |
|---|---|---|---|
| TMP | Trans-membrane pressure (bar) | 1.5 | 4.5 |
| T | Operational temperature (°C) | 25 | 50 |
| CFV | Cross-flow velocity (m/s) | 0.25 | 1.25 |
| pH | pH values | 4 | 10 |
| PFD | Permeation flux decline (L/m$^2$·h) | 65.2 | 212.9 |
| FR | Fouling resistance (m$^{-1}$) | 43.7 | 220.2 |

In this paper, for detection of data integrity violations during storing or transmission of data and modeling of the process, the original experimental data has been displayed [46-48]. For better visualization and proper trend analysis, Fig. 4 shows the three-dimensional plots of experimental dataset used in this study. Also, this figure helps in understanding qualitatively the correlation between these input/output variables. As can be seen in Fig. 4, by increasing pressure, temperature and cross-flow velocity, the amount of permeation flux of PAN membrane during ultrafiltration process is increased, while increasing in the cross-flow velocity causes a decrease in fouling resistance. This decreasing in fouling resistance is consistent with the fact that by increasing the velocity of oily wastewater during ultrafiltration process, the contact time between the oily wastewater and PAN membrane surface increases and thus causes more chemical deposits.

### 2. Model Parameters

In SVM models there are two key parameters: regularization

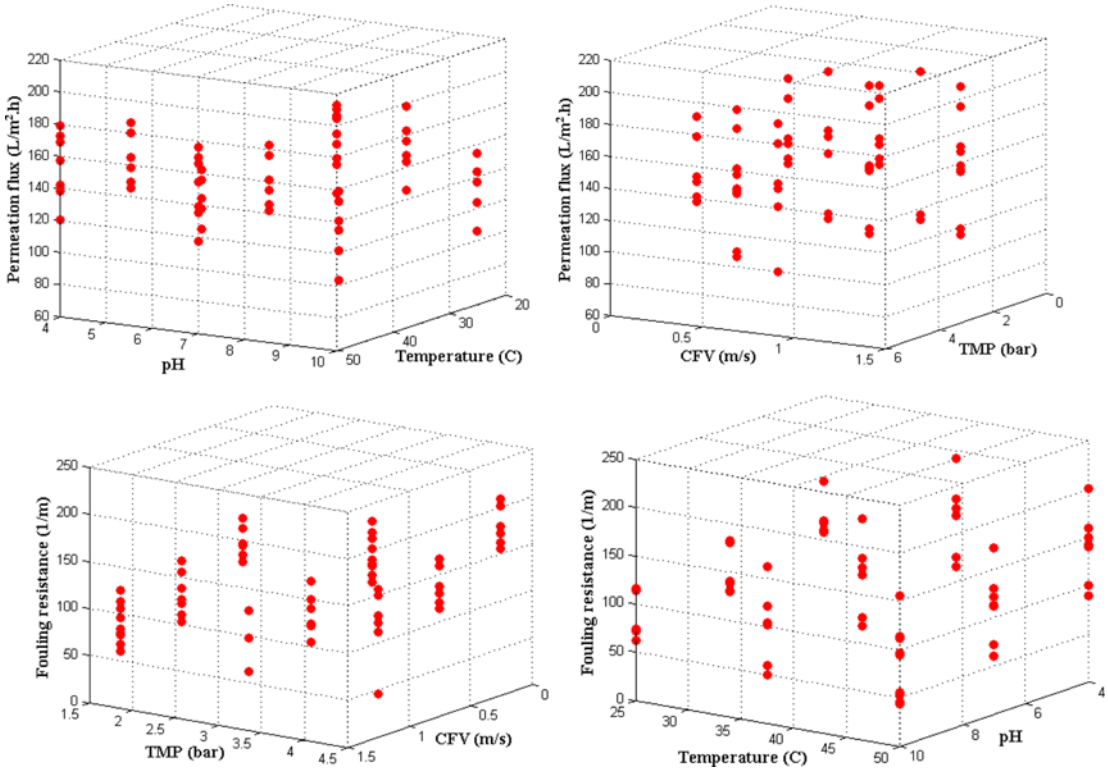


**Fig. 4. Output variables of SVM algorithm versus input parameters.**

**Table 3. The optimum values of the SVM models parameters for output variables**

| Parameters | $\gamma$ | $\sigma^2$ |
|---|---|---|
| Permeation flux decline | 2571 | 2.745 |
| Fouling resistance | 36983 | 6.458 |

parameter ($\gamma$) and kernel parameter ($\sigma^2$). Regularization parameter determines the trade-off between the fitting error minimization and the smoothness of the estimated function, while the kernel parameter plays a crucial role in establishing a good SVM regression model with the high accuracy and stability.

In this study radial basis function (RBF) was used and the kernel-related parameters such as $\gamma$ and $\sigma^2$ were optimized. For this purpose, the optimization toolbox of MATLAB software was used. The number of the population applied for this study was set to 900 to obtain the optimized values of two parameters of SVM-algorithm. To ensure that the value of the final solution is very close to the global optimum of the problem, the optimization procedure was repeated several times. The values of optimized $\gamma$ and $\sigma^2$ are reported in Table 3.

## 3. Model Validation

The experimental data of the present research has been normalized between −1 and +1 to prevent truncation error due to wide ranges of numerical values for input/output variables to be included in the SVM model. Since the model development is based on normalizing data, it is necessary to map input data to a normalized space according to Eq. (10) before the model can be run. Normalized model output should also be mapped into the space of real values for output variable to be compared to experimental data. Two different subsets of data that are necessary to perform model development are training and testing data. Thus the available dataset for permeation flux decline and fouling resistance are divided randomly as explained in Section 4. To develop input/output model the calculation procedures programmed in Matlab environment were executed on an Intel dual-core 2.40 GHz processor accompanied by 4G RAM; it took around 12 hours to get convergence. Convergence indicates that the optimum model is achieved; however, it does not guarantee accuracy of model predictions. To ensure model reliability the input variables of test data subset are entered to the developed model and model predictions are validated against experimental data.

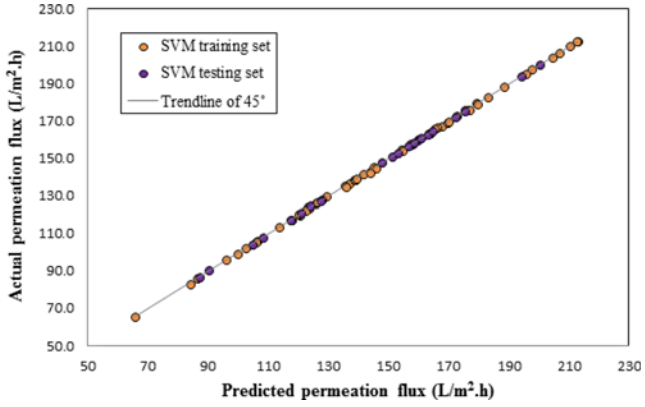


**Fig. 5. Comparison between predicted results of SVM model and actual permeation flux.**

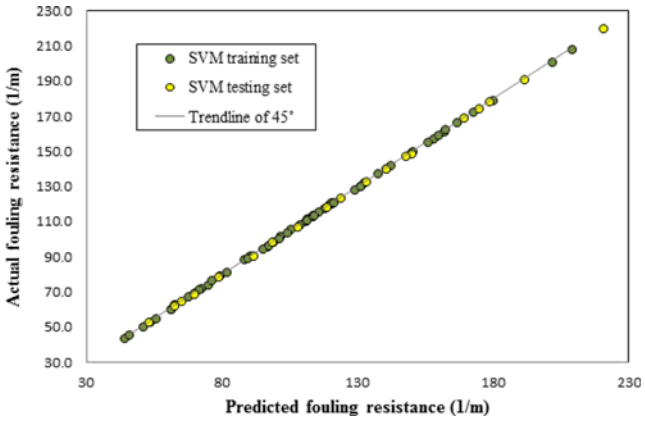


**Fig. 6. Comparison between predicted results of SVM model and actual fouling resistance.**

Figs. 5 and 6 show the actual values of SVM model prediction of permeation flux decline and fouling resistance versus their experimental values for training and testing set, respectively. As indicated in these figures, the SVM-based models predictions follow experimental data in the test process appropriately. This indicates that the SVM model based on universal statistical and optimized algorithm has an exceptionally high capability of capturing nonlinearities.

Performance efficiencies of the SVM-based models of permeation flux decline and fouling resistance were evaluated. Table 4 reports the SVM models performance in terms of mean squared error (MSE) and squared correlation coefficient ($R^2$) between the real targets and SVM results. Also, the accuracy of developed SVM models was calculated using average absolute deviation percent (AAD %), as defined by Eq. (11).

$$\mathrm{AAD\%} = \frac{100}{n}\sum_{i=1}^{n}\left|\frac{y_i - x_i}{y_i}\right| \tag{11}$$

where y, x, and n represent experimental data, model predictions, and number of experimental data points used to calculate AAD%,

**Table 4. Statistical parameters of the presented model for permeation flux decline and fouling resistance**

| Performance | Permeation flux decline | Fouling resistance |
|---|---|---|
| **Training set:** | | |
| MSE | 0.199 | 0.139 |
| AAD% | 0.258 | 0.311 |
| $R^2$ | 0.99 | 0.99 |
| Number of data: | 47 | 47 |
| **Testing set:** | | |
| MSE | 0.074 | 0.069 |
| AAD% | 0.081 | 0.152 |
| $R^2$ | 0.99 | 0.99 |
| Number of data: | 11 | 11 |

respectively. A summary of the calculated AAD% for the developed SVM-based model predictions is presented in Table 4. In brief, the SVM predictions are optimum if $R^2$, AAD% and MSE are found to be close to 1, 0, and 0, respectively.

## CONCLUSION

Support vector machine as a new approach has been used to develop accurate models for prediction/calculation of permeation flux decline and fouling resistance in a cross-flow hydrophilic PAN membrane. The effectiveness of the developed SVM models was also validated by comparing the predicted results with the experimental data. The obtained results from the SVM models show that the proposed method leads to generally acceptable agreement with the investigated experimental data of permeation flux decline and fouling resistance. Also, to evaluate the performance efficiency of the developed models, the numerical values of MSE and AAD% were calculated, which for SVM-based model of permeation flux decline these values were 0.074 and 0.081 for testing set, respectively. Also for fouling resistance these numerical values were 0.069 and 0.152, respectively. This study reveals some application potentials of SVM as a modeling tool in the membrane separation process that requires much more attention to be fully understood.

## ACKNOWLEDGEMENTS

The authors would like to thank Professor Toraj Mohammadi for his helpful comments and suggestion for improving this research.

## REFERENCES

1. M. Cheryan and N. Rajagopalan, *J. Membr. Sci*., **151**, 15 (1998).
2. M. Abbasi, A. Salahi, M. Mirfendereski, T. Mohammadi and A. Pak, *Desalination*, **252**, 113 (2010).
3. P. Srijaroonrat, E. Julien and Y. Aurelle, *J. Membr. Sci*., **159**, 11 (1999).
4. H. Bai, X. Wang, Y. Zhou and L. Zhang, *J. Prog. Nat. Sci*., **250**, 3 (2012).
5. T. Mohammadi, M. Kazemimoghadam and M. Saadabadi, *Desalination*, **157**, 369 (2003).
6. A. Salahi, M. Abbasi and T. Mohammadi, *Desalination*, **251**, 153 (2010).
7. B. Yu, H. Cong and X. Zhao, *J. Prog. Nat. Sci*., **22**, 662 (2012).
8. C. Cheng, J. Uhe, X. Yang, Y. Wu and D. Li, *J. Prog. Nat. Sci*., **22**, 670 (2012).
9. Y. G. Dave and A. V. R. Reddy, *Desalination*, **282**, 9 (2011).
10. D. Yang, X. Zhang, L. Yuan and J. Hu, *J. Prog. Nat. Sci*., **19**, 1305 (2009).
11. J. Xu, X. Feng, P. Chen and C. Gao, *J. Membr. Sci*., **413**, 62 (2012).
12. E. M. V. Hoek, J. Allred, T. Knoell and B. H. Jeong, *J. Membr. Sci*., **314**, 33 (2008).
13. S. C. Tu, V. Ravindran and M. Pirbazari, *J. Membr. Sci*., **265**, 29 (2005).
14. B. Van der Bruggen, M. Manttari and M. Nystrom, *Sep. Purif. Technol*., **63**, 251 (2008).
15. S. F. E. Boerlage, M. D. Kennedy, P. A. C. Bonne, G. Galjaard and J. C. Schippers, *Desalination*, **113**, 231 (1997).
16. N. Yin, S. Chen, Y. Ouyang, L. Tang, J. Yang and H. Wang, *J. Prog. Nat. Sci*., **21**, 472 (2011).
17. S. Ballo, M. Liu, L Hou and J. Chang, *J. Prog. Nat. Sci*., **19**, 873 (2009).
18. S. Gunalan, R. Sivaraj and V. Rajendran, *J. Prog. Nat. Sci*., **22**, 695 (2012).
19. H. Shokrkar, A. Salahi, N. Kasiri and T. Mohammadi, *Chem. Eng. Res. Des*., **90**, 846 (2012).
20. T. M. Hwang, H. Oh, Y. K. Choung, S. Oh, M. Jeon, J. H. Kim, H. N. Nam and S. Lee, *Desalination*, **247**, 285 (2009).
21. Q. F. Liu, S. H. Kim and S. Lee, *Sep. Purif. Technol*., **70**, 96 (2009).
22. S. S. Madaeni and A. R. Kurdian, *Chem. Eng. Res. Des*., **89**, 456 (2011).
23. APHA-American Public Health Association/American Water Works Association/Water Environment Federation, Standard Methods for the Examination of Water and Wastewater, 2001, 20th Ed., Washington DC, USA.
24. S. Rezaei HoseinAbadi, M. R. Sebzari, M. Hemati, F. Rekabdar and T. Mohammadi, *Desalination*, **265**, 222 (2011).
25. T. Mohammadi and A. Esmaeelifar, *J. Membr. Sci*., **254**, 129 (2005).
26. M. A. Hearst, S. T. Dumais, E. Osman, J. Platt and B. Scholkopf, *IEEE Intell. Syst. Appl*., **13**, 18 (1998).
27. M. Schmidt, *Identifying speaker with support vector networks*, In Interface 96 Proceedings, Sydney (1996).
28. N. Cristianini and J. S. Taylor, *An introduction to support vector machine (and other kernel-based learning methods)*, Cambridge Univ. Press, Cambridge (2000).
29. V. N. Vapnik, *Statistical learning theory*, Wiley, New York (1998).
30. M. Pontil and A. Verri, *Neural Comput*., **10**, 955 (1998).
31. A. Eslamimanesh, F. Gharagheizi, M. Illbeigi, A. H. Mohammadi, A. Fazlali and D. Richon, *Fluid Phase Equilib*., **316**, 34 (2012).
32. R. M. Balabin and E. I. Lomakina, *Phys. Chem. Chem. Phys*., **13**, 11710 (2011).
33. J. A. K. Suykens, T. Van Gestel, J. De Brabanter, B. De Moor and J. Vandewalle, Least Squares Support Vector Machines, World Scientific, Singapore (2002).
34. J. A. K. Suykens and J. Vandewalle, *Neural Process. Lett*., **9**, 293 (1999).
35. K. Pelckmans, J. A. K. Suykens, T. Van Gestel, D. De Brabanter, L. Lukas, B. Hamers, B. De Moor and J. Vandewalle, LS-SVMlab: a Matlab/C Toolbox for Least Squares Support Vector Machines, Internal Report 02-44, ESATSISTA, K.U. Leuven, Belgium (2002).
36. V. N. Vapnik, The Nature of Statistical Learning Theory, 2nd Ed. Springer, New York (1995).
37. C. Y. Zhao, H. X. Zhang, X. Y. Zhang, M. C. Liu, Z. D. Hu and B. T. Fan, *Toxicol*., **217**, 105 (2006).
38. X. Peng, *Pattern Recog. Lett*., **44**, 2678 (2011).
39. G. Zanghirati and L. Zanni, *Parallel Comput*., **29**, 535 (2003).
40. J. Terzica, C. R. Nagarajahb and M. Alamgira, *Sens. Actuators*, **161**, 278 (2010).
41. S. Agarwal, V. V. Saradhi and H. Karnick, *Neurocomputing*., **71**, 1230 (2008).
42. R. Strack, V. Kecman, B. Strack and Q. Li, *Neurocomputing*, **59**, 101 (2013).
43. D. C. Li and Y. H. Fang, *Expert. Syst. Appl*., **34**, 2013 (2008).
44. E. Comak and A. Arslan, *Expert. Syst. Appl*., **35**, 564 (2008).

45. J. P. Hwang, S. Park and E. Kim, *Expert. Syst. Appl.*, **38**, 8580 (2011).
46. M. K. Salooki, R. Abedini, H. Adib and H. Koolivand, *Sep. Purif. Technol.*, **1**, 82 (2011).
47. H. Adib, R. Haghbakhsh, M. Saidi, M. A. Takassi, F. Sharifi, M. Koolivand, M. R. Rahimpour and S. Keshtkari, *J. Nat. Gas Sci. Eng.*, **10**, 14 (2013).
48. R. Haghbakhsh, H. Adib, P. Keshavarz, M. Koolivand and S. Keshtkari, *Thermochim. Acta*, **551**, 124 (2013).